Compressive Failure of Fiber Composites: The Roles of Multiaxial Loading and Creep

W. S. Slaughter

N. A. Fleck

Cambridge University Engineering Department, Cambridge CB2 1PZ England

B. Budiansky

Division of Applied Sciences, Harvard University, Cambridge, Massachusetts 02138

The roles of multiaxial loading and creep in compressive failure of aligned fiber composites are considered. Analytical models are developed based on the model given by Budiansky and Fleck (1992). The critical microbuckling stress in multiaxial loading is calculated for a rigid-perfectly plastic solid and an elastic-plastic strain hardening solid. The rigid-perfectly plastic results predict a plane compressive failure surface in stress space. The rigid-perfectly plastic results are sufficiently accurate, when compared to the strain hardening results, so long as the remote shear stress and stress normal to the fiber direction are not too large relative to the remote stress in the fiber direction. The model given for creep microbuckling is suitable for power-law viscous composite behavior. Deformation within a localized kink band is computed as a function of time. A creep life is predicted, based on a critical strain failure criterion.

Introduction

An important failure mechanism for aligned fiber composites in compression in microbuckling. Microbuckling is an event in which the composite suffers localized buckling within a kink band (Hull, 1981). Aligned fiber composites include polymer matrix composites, which are widely used in applications in which the benefits from their high specific tensile moduli and tensile strengths outweigh competing cost considerations, and metal matrix and ceramic matrix composites, which remain largely in the developmental stage. The mechanical properties of metal matrix and ceramic matrix composites are not as well understood as those of polymer matrix composites. Wood, in many circumstances, also behaves as an aligned fiber composite (Dinwoodie, 1981).

A serious limitation for aligned fiber composites is that they often have compressive strengths less than 60 percent of their tensile strengths. The dominant failure mechanism for aligned fiber-polymer matrix composites in compression is microbuckling (Argon, 1972; Budiansky and Fleck, 1992). Microbuckling is also an important failure mechanism in woods (Grossman and Wold, 1971; Dinwoodie, 1981). The role played by microbuckling in the compressive failure of metal matrix and ceramic matrix composites is less clear, though microbuckling has been observed in aluminum alloy matrix composites (Schulte and Minoshima, 1991) and in carbon-carbon composites (Evans and Adler, 1978). Theoretical studies by Argon (1972) and Budiansky and Fleck (1992) have shown that, in polymer matrix components, microbuckling is associated with a nonlinear plastic response of the matrix. The analysis of Budiansky and Fleck (1992) for plastic microbuckling considers the effects of initial imperfections, plastic strain hardening, and combined remote shear stress and axial compression. Here we extend the Budiansky and Fleck (1992) analysis to general multiaxial loading.

Many fiber composites are known to exhibit time *dependent* deformation behavior or creep. These include polymer matrix composites (Horoschenkoff et al., 1988, Ha et al., 1991) and woods (Dinwoodie, 1981). A theoretical analysis assuming linear viscoelastic composite behavior has previously been presented (Slaughter and Fleck, 1992). At elevated temperatures, metal matrix and ceramic matrix composites also creep. An alternative theoretical analysis of creep microbuckling, suitable for power-law viscous composite behavior, is given here.

The structure of this paper is as follows. First, plastic kinking is analyzed for general remote loading. Results are presented for a rigid-perfectly plastic solid and for a strain-hardening deformation theory solid. Creep microbuckling is then addressed for a power law creeping matrix.

General Multiaxial Loading

Microbuckling is characterized by the formation of a kink band in which the aligned fiber composite undergoes localized failure. This kink band is on the order of ten fiber diameters in width and is *not*, in general, normal to the fiber axes. The analysis to follow, for microbuckling under general remote loading, expands upon that given by Budiansky and Fleck (1992). A schematic of the kink band is shown in Fig. 1. The kink band is of width w and forms an angle β with the direction normal to the fiber axes, hereafter called the transverse direction. It is assumed that the fibers are inextensible and that uniform straining within the kink band is associated with a change in fiber orientation, ϕ. It is further assumed that initial

Contributed by the Materials Division and presented at the Symposium on Micromechanics of Ceramics and Ceramic Composites, Winter Annual Meeting, Anaheim, CA, November 8-13, 1992, of the AMERICAN SOCIETY OF MECHANICAL ENGINEERS. Manuscript received by the Materials Division June 20, 1992; revised manuscript received November 30, 1992. Associate Technical Editor: S. Suresh.

misalignment within the composite is represented by the angle $\bar{\phi}$.

Two Cartesian coordinate systems, $(\mathbf{e}_1,\mathbf{e}_2)$ and (ϵ_1,ϵ_2), are defined such that $\mathbf{e}_1$ and $\mathbf{e}_2$ are parallel and normal to the fiber axes outside the kink band, and ϵ_1 and ϵ_2 are parallel and normal to the fiber axes inside the kink band. These two coordinate systems are related by

$$\left.\begin{aligned}\mathbf{e}_1 &= \epsilon_1\cos(\bar{\phi}+\phi)-\epsilon_2\sin(\bar{\phi}+\phi)\\ \mathbf{e}_2 &= \epsilon_2\sin(\bar{\phi}+\phi)+\epsilon_2\cos(\bar{\phi}+\phi)\end{aligned}\right\}. \tag{1}$$

The stress components outside the kink band are defined by

$$\boldsymbol{\sigma}^{\infty} = -\sigma_L^{\infty}\mathbf{e}_1\mathbf{e}_1+\sigma_T^{\infty}\mathbf{e}_2\mathbf{e}_2+\tau^{\infty}(\mathbf{e}_1\mathbf{e}_2+\mathbf{e}_2\mathbf{e}_1) \tag{2}$$

and those within the kink band are defined by

$$\boldsymbol{\sigma} = \sigma_L\epsilon_1\epsilon_1+\sigma_T\epsilon_2\epsilon_2+\tau(\epsilon_1\epsilon_2+\epsilon_2\epsilon_1). \tag{3}$$

In the analysis by Budiansky and Fleck (1992) the remote transverse stress, σ_T^{∞}, was assumed to be zero.

Continuity of Tractions. Continuity of tractions across the kink band interface can be expressed as

$$\mathbf{n}\cdot\boldsymbol{\sigma}^{\infty} = \mathbf{n}\cdot\boldsymbol{\sigma} \tag{4}$$

where $\mathbf{n}=\mathbf{e}_1\cos\beta+\mathbf{e}_2\sin\beta$ is the unit normal to the kink band interface. Equations (1)–(4) lead to the two scalar equations for continuity of tractions in the ϵ_1 and ϵ_2 directions, respectively,

$$-\sigma_L^{\infty}\cos\beta\cos(\bar{\phi}+\phi)+\sigma_T^{\infty}\sin\beta\sin(\bar{\phi}+\phi)+\tau^{\infty}\sin(\beta+\bar{\phi}+\phi) = \sigma_L\cos(\beta-\bar{\phi}-\phi)+\tau\sin(\beta-\bar{\phi}-\phi) \tag{5}$$

$$\sigma_L^{\infty}\cos\beta\sin(\bar{\phi}+\phi)+\sigma_T^{\infty}\sin\beta\cos(\bar{\phi}+\phi)+\tau^{\infty}\cos(\beta+\bar{\phi}+\phi) = \sigma_T\sin(\beta-\bar{\phi}-\phi)+\tau\cos(\beta-\bar{\phi}-\phi) \tag{6}$$

Because the fibers are assumed to be inextensible, the axial stress in the kink band, σ_L, is of no interest in the analysis to follow and Eq. (5) need not be considered further.

It is assumed that the initial misalignment, $\bar{\phi}$, is small. Furthermore, it is anticipated that consideration of small deformation angles, ϕ, will be sufficient to examine the critical events associated with microbuckling. For small $\bar{\phi}+\phi$, linearization of Eq. (6) provides the result

$$(\bar{\phi}+\phi)(\sigma_L^{\infty}\cos\beta-2\tau^{\infty}\sin\beta)\approx(\sigma_T-\sigma_T^{\infty})\sin\beta-(\bar{\phi}+\phi)\sigma_T\cos\beta+(\tau-\tau^{\infty})[\cos\beta+(\bar{\phi}+\phi)\sin\beta]. \tag{7}$$

Equation (7) can be further approximated, when $[(\pi/2)-\beta \gg 0]$, by dropping the term $(\tau-\tau^{\infty})(\bar{\phi}+\phi)\sin\beta$ from the right-hand side, to give

$$\sigma_L^{\infty}-2\tau^{\infty}\tan\beta\approx\frac{\tau-\tau^{\infty}+(\sigma_T-\sigma_T^{\infty})\tan\beta}{\bar{\phi}+\phi}-\sigma_T. \tag{8}$$

This form of the approximation is chosen so that, when the composite behaves elastically, a proper account of the terms involving the remote stresses is maintained. This will be shown explicitly later.

Kinematic Relations. Kinematic conditions for kink band deformation are now examined. Consider a material point P within the kink band. The position vector $\mathbf{r}$ to point P is

$$\mathbf{r} = \xi_1\epsilon_1+\xi_2\epsilon_2 = y(-\mathbf{e}_1\tan\beta+\mathbf{e}_2)+x\epsilon_1 \tag{9}$$

where the scalar lengths ξ_1, ξ_2, x, and y are defined as shown in Fig. 1 and related by

$$\left.\begin{aligned}x &= \xi_1+\xi_2\tan(\beta-\bar{\phi}+\phi)\\ y &= \xi_2\cos\beta\sec(\beta-\bar{\phi}+\phi)\end{aligned}\right\}. \tag{10}$$

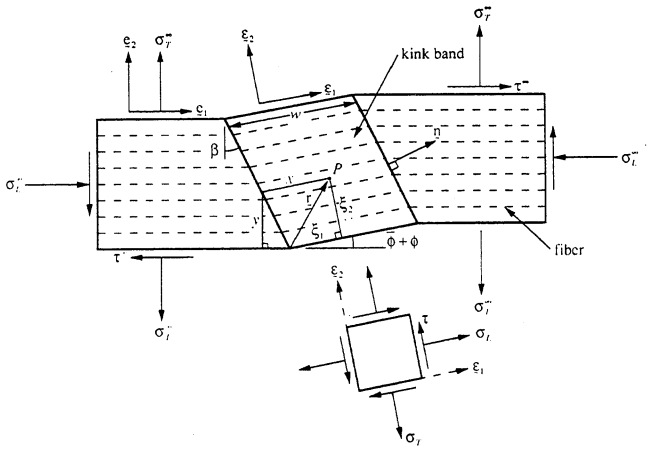

Fig. 1 Schematic of microbuckling kink band in an aligned fiber composite, showing parameters and sign conventions

The velocity of point P is

$$\mathbf{v} = y\dot{\gamma}^{\infty}\mathbf{e}_1+y\dot{e}_T^{\infty}\mathbf{e}_2+x\dot{\phi}\epsilon_2 \tag{11}$$

where $\dot{\gamma}^{\infty}$ and $\dot{e}_T^{\infty}$ are, respectively, the shear strain rate and transverse strain rate outside the kink band and $\dot{f}(t)\equiv df(t)/dt$. In the analysis by Budiansky and Fleck (1992), the remote transverse strain rate, $\dot{e}_T^{\infty}$, was zero.

The strain rate tensor within the kink band is related to the velocity field by

$$\dot{\boldsymbol{\epsilon}} = \frac{1}{2}[\nabla\mathbf{v}+(\nabla\mathbf{v})^T] \tag{12}$$

where the superscript T denotes the transpose, and the gradient operator ∇ is

$$\nabla = \epsilon_1\frac{\partial}{\partial\xi_1}+\epsilon_2\frac{\partial}{\partial\xi_2}. \tag{13}$$

With the strain rate components within the kink band defined by

$$\dot{\boldsymbol{\epsilon}} = \dot{e}_T\epsilon_2\epsilon_2+\frac{1}{2}\dot{\gamma}(\epsilon_1\epsilon_2+\epsilon_2\epsilon_1), \tag{14}$$

Eq. (12), along with Eqs. (1) and (9)–(11), gives the kinematic conditions

$$\left.\begin{aligned}\dot{e}_T &= \dot{\phi}\tan(\beta-\bar{\phi}-\phi)+[\dot{e}_T^{\infty}\cos(\bar{\phi}+\phi)-\dot{\gamma}^{\infty}\sin(\bar{\phi}+\phi)]\cos\beta\sec(\beta-\bar{\phi}-\phi)\\ \dot{\gamma} &= \dot{\phi}+[\dot{\gamma}^{\infty}\cos(\bar{\phi}+\phi)+\dot{e}_T^{\infty}\sin(\bar{\phi}+\phi)]\cos\beta\sec(\beta-\bar{\phi}-\phi)\end{aligned}\right\}. \tag{15}$$

Differentiating Eq. (9), and noting that $\dot{\mathbf{r}}=\mathbf{v}$, $\dot{y}=y\dot{e}_T^{\infty}$, and $\dot{\epsilon}_1=\dot{\phi}\epsilon_2$, it follows from Eq. (11) that

$$\dot{\beta} = -(\dot{e}_T^{\infty}\sin\beta+\dot{\gamma}^{\infty}\cos\beta)\cos\beta. \tag{16}$$

For $\bar{\phi}+\phi$, e_T^{∞}, and γ^{∞} small, Eqs. (15) and (16) reduce to the approximate kinematic equations

$$\left.\begin{aligned}e_T &\approx e_T^{\infty}+\phi\tan\beta\\ \gamma &\approx \gamma^{\infty}+\phi\\ \beta &\approx \beta_0\end{aligned}\right\} \tag{17}$$

where β_0 is the kink band angle associated with zero remote straining.

Constitutive Relations. If the composite deforms elastically, then the kinematic conditions, Eqs. (17), lead to

$$\left.\begin{aligned}\sigma_T &\approx \sigma_T^{\infty}+E_T\phi\tan\beta\\ \tau &\approx \tau^{\infty}+G\phi\end{aligned}\right\} \tag{18}$$

where E_T and G, respectively, are the transverse and shear elastic moduli for the composite. The *exact* equation for continuity of tractions, Eq. (6), combined with this result and then linearized gives the approximate elastic kink band response

$$\sigma_L^\infty + \sigma_T^\infty - 2\tau^\infty \tan\beta \approx [G + E_T \tan^2\beta] \frac{\phi}{\bar{\phi}+\phi}. \tag{19}$$

An examination of Eq. (8), the *approximate* equation for continuity of tractions, shows that it also reduces to the correct result for elastic kink band response, Eq. (19).

The following constitutive equations for plastic deformation have previously been derived by Budiansky and Fleck (1992) and, unlike the equations for continuity of tractions and the kinematic conditions, are unchanged by the consideration of general multiaxial loading. Consequently, the derivation is only outlined here. Assume that the composite is characterized by the quadratic yield condition

$$\left(\frac{\tau_e}{\tau_y}\right)^2 = \left(\frac{\tau}{\tau_y}\right)^2 + \left(\frac{\sigma_T}{\sigma_{Ty}}\right)^2 \tag{20}$$

where τ_y and σ_{Ty} are the plane strain yield stresses in pure shear and pure transverse tension in the case of perfect plasticity (when $\tau_e = \tau_y$, a constant). The effective stress, τ_e, which can be rewritten as

$$\tau_e \equiv \sqrt{\tau^2 + (\sigma_T/R)^2}, \tag{21}$$

is used as a plastic potential for the plastic strain rates, $\dot{\gamma}^p$ and $\dot{e}_T^p$. The parameter $R = \sigma_{Ty}/\tau_y$ defines the eccentricity of the yield ellipse which expands homogeneously with increasing τ_e due to strain hardening.

Discounting the possibility of elastic unloading, the associated flow theory relations for plastic strain rates, based on τ_e as a plastic potential, can be written as

$$\left.\begin{aligned} \dot{\gamma}^p &= F(\tau_e)\frac{\partial \tau_e}{\partial \tau}\dot{\tau}_e \\ \dot{e}_T^p &= F(\tau_e)\frac{\partial \tau_e}{\partial \sigma_T}\dot{\tau}_e \end{aligned}\right\}. \tag{22}$$

where $F(\tau_e)$ is a measure of the rate of strain hardening. A work-equivalent effective plastic strain rate, $\dot{\gamma}_e^p$, is defined by

$$\tau\dot{\gamma}^p + \sigma_T \dot{e}_T^p = \tau_e \dot{\gamma}_e^p \tag{23}$$

and it follows that

$$\dot{\gamma}_e^p = F(\tau_e)\dot{\tau}_e = \sqrt{(\dot{\gamma}^p)^2 + R^2(\dot{e}_T^p)^2}. \tag{24}$$

Thus, we interpret $F(\tau_e)$ as the inverse of the tangent modulus in pure shear. Substituting Eq. (24) into Eq. (22) and assuming proportional loading leads to

$$\left.\begin{aligned} \gamma^p &= \left(\frac{\gamma_e^p}{\tau_e}\right)\tau \\ e_T^p &= \left(\frac{\gamma_e^p}{\tau_e}\right)\frac{\sigma_T}{R^2} \\ \gamma_e^p &= \sqrt{(\gamma^p)^2 + R^2(e_T^p)^2} \end{aligned}\right\}. \tag{25}$$

Note that the functional dependence of γ_e^p on τ_e must be the same as that of γ^p on τ for pure shear. Equations (25) have the form of a *deformation theory* of plasticity. Since microbuckling is a plastic buckling phenomenon, and deformation theories are known to give more accurate predictions to plastic buckling problems than flow theories, we adopt a deformation theory of plasticity and use Eqs. (25) in the remainder of the paper, even though proportional loading may not always be maintained. The microbuckling stress is now derived for the rigid-perfectly plastic solid, and then for a Ramberg-Osgood strain hardening solid.

Rigid-Perfectly Plastic Solid. Assume that the composite behaves in a rigid-perfectly plastic manner, with plastic yielding within the kink band only. The elastic components of strain vanish and the constitutive Eqs. (25) can be combined with the approximate kinematic Eqs. (17) to give, after eliminating γ_e^p,

$$\sigma_T \approx \tau R^2 \tan\beta. \tag{26}$$

Combining Eq. (26) with the yield condition, Eq. (20) (with $\tau_e/\tau_y = 1$), yields

$$\tau \approx \tau_y/\alpha \tag{27}$$

where

$$\alpha \equiv \sqrt{1 + R^2\tan^2\beta}. \tag{28}$$

Finally, the rigid-perfectly plastic load response of the kink band is obtained by substituting Eqs. (26) and (27) into the approximate expression for continuity of tractions across the kink band interface, Eq. (8),

$$\sigma_L^\infty \approx \frac{\alpha\tau_y - \tau^\infty - \sigma_T^\infty\tan\beta}{\bar{\phi}+\phi} - \frac{1}{\alpha}\tau_y R^2\tan\beta + 2\tau^\infty\tan\beta. \tag{29}$$

Since $\bar{\phi}+\phi$ is small, the expression can be further approximated by dropping the last two terms, leaving

$$\sigma_L^\infty \approx \frac{\alpha\tau_y - \tau^\infty - \sigma_T^\infty\tan\beta}{\bar{\phi}+\phi}. \tag{30}$$

Equation (30) reduces to the solution given by Fleck and Budiansky (1991) when there is zero transverse stress outside the kink band, $\sigma_T^\infty = 0$.

The critical microbuckling stress, $(\sigma_L^\infty)_c$, for an applied constant remote shear and transverse stresses, τ^∞ and σ_T^∞, is given by Eq. (30) when $\phi = 0$. Both the remote shear stress and the remote transverse stress reduce the critical microbuckling stress in a linear fashion. The microbuckling stress is inversely proportional to the initial imperfection $\bar{\phi}$. Note that when $\beta = 0$ the remote transverse stress ceases to affect microbuckling when the composite is a rigid-perfectly plastic solid.

Strain-Hardening Solid. Consider the case where the composite behaves as an elastic-plastic strain-hardening solid. As previously noted, the functional dependence of γ_e^p on τ_e is assumed to equal that of γ^p on τ in pure shear, so that

$$\gamma_e^p = \left[\frac{1}{G_s(\tau_e)} - \frac{1}{G}\right]\tau_e \tag{31}$$

where the function $G_s(\tau_e)$ is the pure shear secant modulus. Combining the elastic and plastic strain components from Eq. (25), using Eq. (31), and, for simplicity, imposing the arbitrary condition

$$\frac{E_T}{G} = R^2 = \left(\frac{\sigma_{Ty}}{\tau_y}\right)^2, \tag{32}$$

leads to

$$\left.\begin{aligned} \gamma &= \frac{\tau}{G} + \gamma^p = \left(\frac{1}{G} + \frac{\gamma_e^p}{\tau_e}\right)\tau = \frac{\tau}{G_s(\tau_e)} \\ e_T &= \frac{\sigma_T}{E_T} + e_T^p = \left[\frac{1}{E_T} + \frac{1}{R^2}\left(\frac{\gamma_e^p}{\tau_e}\right)\right]\sigma_T = \frac{\sigma_T}{R^2 G_s(\tau_e)} \end{aligned}\right\}. \tag{33}$$

A total effective strain is defined by

$$\gamma_e \equiv \frac{\tau_e}{G_s(\tau_e)} \tag{34}$$

so that

$$\gamma_e = \sqrt{\gamma^2 + R^2 e_T^2} = \gamma_e^p + \frac{\tau_e}{G}. \tag{35}$$

Thus, γ_e is the sum of an elastic part, τ_e/G, and a plastic part,

γ_e^p, defined in Eq. (25). Equations (33) can be rewritten simply as

$$\left.\begin{aligned}\gamma &= \left(\frac{\gamma_e}{\tau_e}\right)\tau \\ e_T &= \left(\frac{\gamma_e}{\tau_e}\right)\frac{\sigma_T}{R^2}\end{aligned}\right\}. \tag{36}$$

The three parameter (G,τ_y,n) Ramberg-Osgood representation is used to explicitly implement constitutive equations in this paper. With τ_y defined as the stress at which the secant modulus is equal to 70 percent of the elastic modulus, i.e., $G_s(\tau_y)=0.7G$, the Ramberg-Osgood representation for pure shear of the *composite* is

$$\frac{\gamma}{\gamma_y}=\frac{\tau}{\tau_y}+\frac{3}{7}\left(\frac{\tau}{\tau_y}\right)^n \tag{37}$$

where $\gamma_y \equiv \tau_y/G$ is the elastic component of strain at $\tau=\tau_y$. Also, the secant modulus $G_s(\tau)$ is given by

$$\frac{G}{G_s(\tau)}=1+\frac{3}{7}\left(\frac{\tau}{\tau_y}\right)^{n-1}. \tag{38}$$

The Ramberg-Osgood representation reduces to the elastic representation when $\tau_y \to \infty$ and gives the elastic-perfectly plastic response when $n \to \infty$. The relations are applied to Eqs. (31)–(36) by replacing τ and γ with τ_e and γ_e.

Combining continuity of tractions, Eq. (8), with the kinematic constraints, Eqs. (17), and the constitutive Eqs. (36) leads to

$$\sigma_L^\infty - 2\tau^\infty\tan\beta = \frac{(\alpha^2\phi+\gamma^\infty+R^2 e_T^\infty\tan\beta)\dfrac{\tau_e}{\gamma_e}-\tau^\infty-\sigma_T^\infty\tan\beta}{\bar{\phi}+\phi} - R^2(e_T^\infty+\phi\tan\beta)\frac{\tau_e}{\gamma_e} \tag{39}$$

where

$$\gamma_e^2=\alpha^2\phi^2+R^2[(e_T^\infty)^2+2e_T^\infty\phi\tan\beta]+2\gamma^\infty\phi+(\gamma^\infty)^2 \tag{40}$$

and α has been previously defined in Eq. (28). Define the following nondimensional parameters: $t\equiv\tau_e/\tau_y$, $\eta\equiv\gamma_e/\gamma_y$, $t^\infty\equiv\tau^\infty/\tau_y$, $\eta^\infty\equiv\gamma^\infty/\gamma_y$, $s^\infty\equiv\sigma_T^\infty/\tau_y$, $\epsilon^\infty\equiv e_T^\infty/\gamma_y$, $\omega\equiv\phi/\gamma_y$, $\bar{\omega}\equiv\bar{\phi}/\gamma_y$. Equations (39) and (40) may now be rewritten in nondimensional form,

$$A\equiv\frac{\sigma_L^\infty-2\tau^\infty\tan\beta}{G}=\frac{(\alpha^2\omega+\eta^\infty+R^2\epsilon^\infty\tan\beta)\dfrac{t}{\eta}-t^\infty-s^\infty\tan\beta}{\bar{\omega}+\omega} - |\gamma_y e|R^2(\epsilon^\infty+\omega\tan\beta)\frac{t}{\eta} \tag{41}$$

$$\eta=\sqrt{\alpha^2\omega^2+R^2[(\epsilon^\infty)^2+2\epsilon^\infty\omega\tan\beta]+2\eta^\infty\omega+(\eta^\infty)^2}. \tag{42}$$

The critical microbuckling load is achieved when $dA/d\omega=0$. Setting $dA/d\omega=0$ leads to the parametric equations

$$A_c=\alpha^2\frac{dt}{d\eta}+\left(\frac{t}{\eta}-\frac{dt}{d\eta}\right)\left(\frac{\eta^\infty}{\eta}\right)^2\left[\alpha^2-1+R^2\left(\frac{\epsilon^\infty}{\eta^\infty}\right)^2-2R^2\frac{\epsilon^\infty}{\eta^\infty}\tan\beta\right]-\gamma_y R^2(\bar{\omega}\tan\beta+\epsilon^\infty+2\omega\tan\beta)\frac{t}{\eta}+\gamma_y\frac{R^2}{\eta^2}(\alpha^2\omega+R^2\epsilon^\infty\tan\beta+\eta^\infty)(\epsilon^\infty+\omega\tan\beta)(\bar{\omega}+\omega)\left(\frac{t}{\eta}-\frac{dt}{d\eta}\right) \tag{43}$$

$$\bar{\omega}=\frac{(\alpha^2\omega+\eta^\infty+R^2\epsilon^\infty\tan\beta)\dfrac{t}{\eta}-t^\infty-s^\infty\tan\beta-\gamma_y R^2\omega(\epsilon^\infty+\omega\tan\beta)\dfrac{t}{\eta}-\omega A_c}{A_c+\gamma_y R^2(\epsilon^\infty+\omega\tan\beta)\dfrac{t}{\eta}} \tag{44}$$

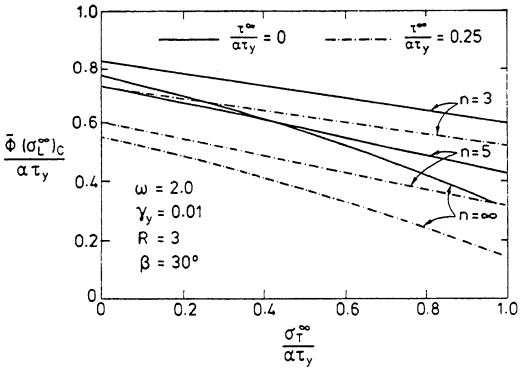

Fig. 2 The critical microbuckling stress versus the remote transverse stress from the Ramberg-Osgood strain-hardening analysis, for $\beta=30$ deg

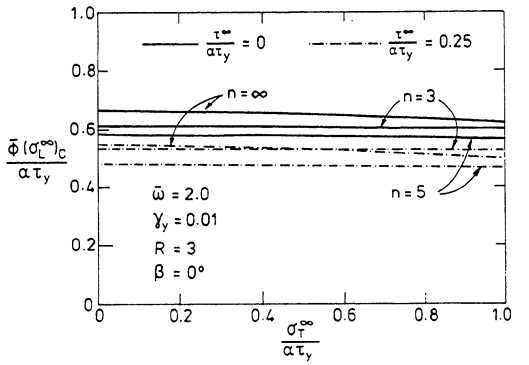

Fig. 3 The critical microbuckling stress versus the remote transverse stress from the Ramberg-Osgood strain-hardening analysis, for $\beta=0$ deg

where $A_c\equiv[(\sigma_L^\infty)_c-2\tau^\infty\tan\beta]/G$. To generate solutions for the microbuckling stress $(\sigma_L^\infty)_c$ for given constant values of t^∞ and s^∞ (and, therefore, η^∞ and ϵ^∞), first assume a value for the kink band deformation angle, ω, at maximum load and calculate the corresponding effective strain, η, from Eq. (42). Use the constitutive relations, e.g., the Ramberg-Osgood Eq. (37), to calculate, numerically if necessary, the effective stress, t, and its first derivative, $dt/d\eta$. A good initial guess for A_c is given by Eq. (43) without the terms involving γ_y. Equations (43) and (44) can then be solved iteratively for A_c and $\bar{\omega}$ and, thus, $(\sigma_L^\infty)_c$.

In the elastic-perfectly plastic limit of the Ramberg-Osgood relation, when $n\to\infty$, there exists a transition value of initial imperfection, $\bar{\omega}_T$, such that for $\bar{\omega}<\bar{\omega}_T$ the maximum value of A is obtained at initial yield. In this case, $t=\eta=1$ and A_c is given by Eq. (41). Otherwise, if $\bar{\omega}>\bar{\omega}_T$, the previously described procedure is followed with $t=1$ and $dt/d\eta=0$. For a more detailed discussion, see Budiansky and Fleck (1992).

The critical microbuckling stress is shown as a function of the remote transverse stress in Figs. 2 and 3. Results are given for different values of the remote shear stress, Ramberg-Osgood parameter, n, and kink band angle, β. There is a strong dependence of the microbuckling stress $(\sigma_L^\infty)_c$ on the remote shear stress τ^∞ and a weaker dependence on remote transverse stress σ_T^∞. Note that when $\beta=0$ the dependence on remote transverse stress nearly vanishes. This agrees with the results from the rigid-perfectly plastic analysis. The ratio of the strain hardening results to the rigid-perfectly plastic results are plot-

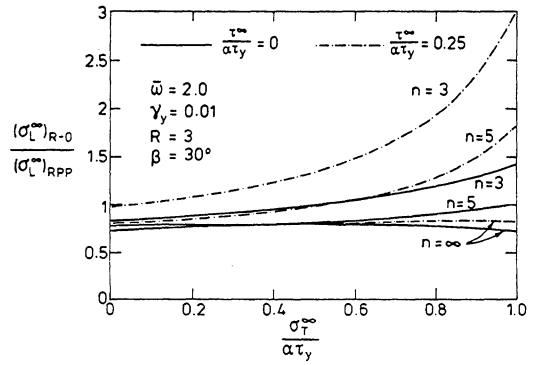

Fig. 4 Ratio of the critical microbuckling results from the Ramberg-Osgood strain-hardening analysis to the results from the rigid-perfectly plastic analysis as a function of the remote transverse stress, for $\beta = 30$ deg

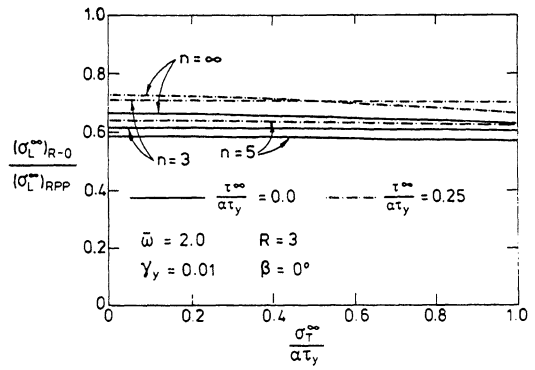

Fig. 5 Ratio of the critical microbuckling results from the Ramberg-Osgood strain-hardening analysis to the results from the rigid-perfectly plastic analysis as a function of the remote transverse stress, for $\beta = 0$ deg

ted in Figs. 4 and 5. This comparison is intended to assess the accuracy of the simple, analytical rigid-perfectly plastic result, Eq. (30). There is considerable variability with Ramberg-Osgood parameter, n, but when the remote shear stress and remote transverse stress are not too large the rigid-perfectly plastic result, Eq. (30), gives acceptable results.

Creep Microbuckling

In the following creep microbuckling analysis, it is presumed that under a state of constant remote stress, localized deformation within a kink band proceeds as a function of time. The conventions and assumptions of the previous section are retained to describe the state of stress, strain, and deformation of the composite (Fig. 1). For a given general multiaxial loading, $\boldsymbol{\sigma}^\infty$, and initial imperfection, $\bar{\phi}$, fibers rotate in the kink band with increasing time. The function $\phi(t)$ is sought.

Failure is associated with debonding of the fiber-matrix interface, matrix microbuckling, or with other mechanisms which result in a sharp decrease in the load bearing ability of the kink band. The failure criterion proposed by Slaughter and Fleck (1992) will be used here. This criterion is based on the quadratic condition

$$\left(\frac{e_T}{e_{Tf}}\right)^2+\left(\frac{\gamma}{\gamma_f}\right)^2=1 \tag{45}$$

where e_{Tf} is the transverse failure strain and γ_f is the shear failure strain. Assuming that $e_{Tf} \ll \gamma_f$, then the failure criterion simplifies to

$$e_T \approx e_{Ff}. \tag{46}$$

For the purposes of this paper, $e_{Tf}=0.01$ or 0.02.

Assume that the effective stress, τ_e, defined in Eq. (21) can be used as a creep potential, so that

$$\left.\begin{aligned}\dot{\gamma}&=H(\tau_e)\frac{\partial\tau_e}{\partial\tau}\\ \dot{e}_T&=H(\tau_e)\frac{\partial\tau_e}{\partial\sigma_T}\end{aligned}\right\}. \tag{47}$$

Let $\dot{\gamma}_e$ be a work rate conjugate of τ_e defined by

$$\tau\dot{\gamma}+\sigma_T\dot{e}_T=\tau_e\dot{\gamma}_e \tag{48}$$

from which it follows that

$$\dot{\gamma}_e=H(\tau_e). \tag{49}$$

Using Eqs. (21) and (47)–(49) leads to

$$\left.\begin{aligned}\dot{\gamma}&=\frac{\tau}{\tau_e}\dot{\gamma}_e\\ \dot{e}_T&=\frac{\sigma_T}{R^2\tau_e}\dot{\gamma}_e\end{aligned}\right\} \tag{50}$$

and

$$\dot{\gamma}_e=\sqrt{\dot{\gamma}^2+R^2\dot{e}_T^2}. \tag{51}$$

The analysis is simplified if one considers only pure axial compression ($\sigma_T^\infty=\tau^\infty=0$). In this case the kink band angle, β, is constant and the kinematic conditions can be expressed approximately, for small $\bar{\phi}+\phi$, as

$$\left.\begin{aligned}\dot{e}_T&\approx\dot{\phi}\tan\beta\\ \dot{\gamma}&=\dot{\phi}\end{aligned}\right\}, \tag{52}$$

which along with Eq. (51) leads to the expression for the effective strain rate, $\dot{\gamma}_e$, in terms of $\dot{\phi}$,

$$\dot{\gamma}_e=\alpha\dot{\phi} \tag{53}$$

where α has been previously defined in Eq. (28). In the expression for continuity of tractions, Eq. (8), the last term on the right-hand side can be neglected, since $\bar{\phi}+\phi$ is assumed small. This, along with Eqs. (50), (52), and (53), leads to an expression for the effective stress, τ_e, in terms of the axial compressive stress, σ_L^∞,

$$\tau_e\approx\frac{1}{\alpha}(\bar{\phi}+\phi)\sigma_L^\infty. \tag{54}$$

It is assumed that the creep behavior is described by the functional relation

$$\dot{\gamma}_e=g(\tau_e) \tag{55}$$

where $g(\tau_e)$ is an unspecified function of τ_e. Thus the deformation rate, $\dot{\phi}$, is related to the deformation, ϕ, and axial load, σ_L^∞, by

$$\dot{\phi}=\frac{1}{\alpha}g\left[\frac{1}{\alpha}(\bar{\phi}+\phi)\sigma_L^\infty\right]. \tag{56}$$

Let ϕ_f be the kink band deformation angle at failure, i.e., when Eq. (46) is satisfied. Integration of Eq. (52) gives the relation between ϕ_f and e_{Tf},

$$\phi_f\approx\frac{e_{Tf}}{\tan\beta}. \tag{57}$$

The failure time t_f, or creep life, is deduced by integrating Eq. (56) from $\phi=0$ at $t=0$ to $\phi=\phi_f$ at $t=t_f$, giving

$$t_f=\int_0^{\phi_f}\frac{\alpha}{g\left[\frac{1}{\alpha}(\bar{\phi}+\phi)\sigma_L^\infty\right]}\,d\phi. \tag{58}$$

One possible form of creep behavior is that of a power-law viscous solid,

$$\tau_e=\tau_0\dot{\gamma}_e^m \tag{59}$$

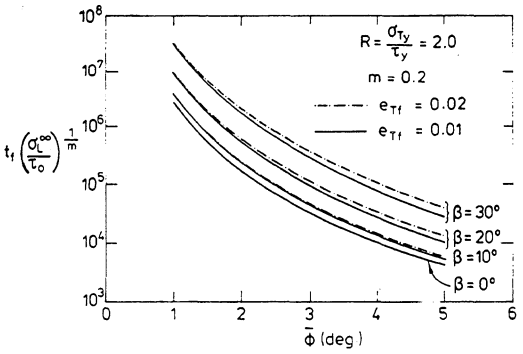

Fig. 6 Creep life as a function of fiber waviness and kink band inclination, for a power-law viscous material

where τ_0 and m (with $m<1$) are material properties. In this case, $g(\tau_e)=(\tau_e/\tau_0)^{1/m}$, which when inserted into Eq. (58) yields

$$t_f=\alpha^{\frac{m+1}{m}}\left(\frac{m}{1-m}\right)\left(\frac{\tau_0}{\sigma_L^\infty}\right)^{\frac{1}{m}}\left[\frac{-}{\phi}^{\frac{m-1}{m}}-(\bar{\phi}+\phi_f)^{\frac{m-1}{m}}\right] \quad (60)$$

as the creep life.

The creep life t_f is shown as a function of $\bar{\phi}$, β, and e_{Tf} in Fig. 6 for the power-law viscous solid. Note that t_f scales with σ_L^∞ as $(\sigma_L^\infty)^{-1/m}$; also, t_f decreases rapidly with increasing $\bar{\phi}$ and decreasing β. That t_f decreases with decreasing β is due solely to the β dependence of α. The tendency of the β dependence of ϕ_f to increase t_f with decreasing β is comparatively small. Most of the creep life is spent with ϕ close to $\bar{\phi}$: the creep life is relatively insensitive to the magnitude of e_{Tf}. When $\beta=0$ the approximate equation for the kink band deformation angle at failure ϕ_f, Eq. (57), is no longer appropriate. However, provided $\bar{\phi}$ is small, the creep life t_f in this case is approximated by Eq. (60) without the term involving $(\bar{\phi}+\phi_f)$ and is independent of e_{Tf}.

Concluding Discussion

The microbuckling analysis presented in this paper follows the collapse response of an imperfect structure. It is not a bifurcation analysis. The effects of fiber bending stiffness are neglected, with the result that there is no length scale in the analysis. The neglect of fiber bending stiffness is a valid approximation (Budiansky et al., 1992). Fibers are implicitly assumed to be broken at the kink band interface, but without fiber bending stiffness this is not an issue.

The critical stress state for microbuckling of a rigid-perfectly plastic solid is given by Eq. (30), with $\phi=0$. This failure criterion defines a plane in $(\sigma_L^\infty,\sigma_T^\infty,\tau^\infty)$ space, and serves as a useful engineering guide-line for the significance of plastic kinking under multiaxial loading. It is noted that the axial microbuckling stress $(\sigma_L^\infty)_c$ is sensitive to the degree of fiber waviness $\bar{\phi}$. As a rough guide, we deduce from Eq. (30) that plastic microbuckling is an important mechanism in the compressive failure of unidirectional aligned fiber composites when the in-plane shear strength of the composite τ_y is significantly less then the axial compressive stress associated with fiber crushing, σ_f, times the fiber waviness $\bar{\phi}$, i.e., $\tau_y<\bar{\phi}\sigma_f$. Consider the case of ceramic matrix and metal matrix composites, reinforced with ceramic fibers such as silicon carbide or carbon. The axial strength of unidirectional material associated with fiber compressive fracture is of the order of $\sigma_f=2000$ MPa. A fiber misalignment angle $\bar{\phi}$ of 3 deg is assumed. Then, the criterion $\tau_y<\bar{\phi}\sigma_f$ implies that microbuckling is expected, in ceramic matrix and metal matrix composites, when the composite has a shear strength of less than 100 MPa. This is the case for ceramic matrix composites which are severely microcracked during processing. The above argument is unaffected by the degree of fiber-matrix debonding. The effect of fiber debonding is to reduce the shear strength to approximately $v_m\tau_y$, where v_m is the matrix volume fraction.

Little is known about the compressive creep behavior of ceramic matrix and metal matrix composites. The analysis given in this paper suggests that creep microbuckling becomes of concern when the in-plane shear creep rate of the composite is appreciable at a shear stress of the order $\bar{\phi}\sigma_f$. For the purposes of the discussion assume a kink band angle $\beta=0$. Then material in the kink band suffers simple shear at a rate $\dot{\gamma}=\dot{\phi}$. Assuming that the creep life is governed by the initial rotation rate of material in the kink band, then $\dot{\phi}\approx\phi_f/t_f$ when ϕ_f is the fiber rotation at failure and t_f is the creep life.

Thus creep microbuckling is expected when the in-plane creep response of the composite under shear is such that the creep rate $\dot{\gamma}$ is of the order ϕ_f/t_f at a shear stress of $\bar{\phi}\sigma_f$. Again taking some approximate values for a metal matrix or ceramic matrix composite, $\phi_f=5$ deg, $\bar{\phi}=3$ deg, $\sigma_f=2000$ MPa, then for a creep life t_f of 100 hours, the composite must creep at a rate $\dot{\gamma}$ of as little as 10^{-7} s^{-1} under an in-plane shear stress of 100 MPa. It is thought that such creep rates are achievable even at only moderate temperatures. Therefore, creep microbuckling is of potential concern in the design of metal matrix and ceramic matrix composites.

Acknowledgments

The authors are grateful for financial support from the ONR, contract 0014-91-J-1916, and from the Procurement Executive of the Ministry of Defence, contract 2029/267.

References

Argon, A. S., 1972, "Fracture of Composites," *Treatise of Materials Science and Technology*, Vol. 1, Academy Press, New York.

Budiansky, B., Deng, L., and Fleck, N. A., 1992, "Predictions of the Kink Width in Fiber Composites," to be submitted to *J. Mech. Phys. Solids.*

Budiansky, B., and Fleck, N. A., 1992, "Compressive Failure of Fiber Composites," to appear in *J. Mech. Phys. Solids.*

Dinwoodie, J. M., 1981, *Timber: Its Nature and Behavior*, Van Nostrand Reinhold Company, Berkshire, England.

Evans, A. G., and Adler, W. F., 1978, "Kinking as a Mode of Structural Degradation in Carbon Fiber Composites," *Acta Metallurgica*, Vol. 26, pp. 725–738.

Fleck, N. A., and Budiansky, B., 1991, "Compressive Failure of Fiber Composites Due to Microbuckling," *Proc. IUTAM Symp. on Inelastic Deformation of Composite Materials*, Troy, NY, May 29–June 1, 1990, ed., J. Dvorak, Springer-Verlag, pp. 235–273.

Grossman, P. U. A., and Wold, M. B., 1971, "Compressive Fracture of Wood Parallel to the Grain," *Wood Sci. Tech.*, Vol. 5, pp. 147–156.

Ha, S. K., Wang, Q., and Chang, F., 1991, "Modeling the Viscoplastic Behavior of Fiber-Reinforced Thermoplastic Matrix Composites at Elevated Temperatures," *J. Comp. Mat.*, Vol. 25, pp. 335–373.

Horoschenkoff, A., Brandt, J., Warnecke, J., and Brüller, O. S., 1988, "Creep Behavior of Carbon Fiber Reinforced Polyetheretherketone and Epoxy Resin," *New Generation Materials and Processes*, Milan.

Hull, D., 1981, *An Introduction to Composite Materials*, Cambridge University Press, Cambridge.

Schulte, K., and Minoshima, K., 1991, "Mechanisms of Fracture and Failure in Metal Matrix Composites," *12th Riso. Int. Symp. on Materials Science: Metal Matrix Composites Processing, Microstructure, and Properties*, ed., N. Hansen et al., pp. 123–147.

Slaughter, W. S., and Fleck, N. A., 1992, "Viscoelastic Microbuckling of Fiber Composites,"submitted for publication to ASME *Journal of Applied Mechanics*.